.

Impact of Casson Fluid on Magneto hydrodynamical multifluid flow under the influence of chemical reaction

Shreedevi Kalyan[1], Indrajeeth reddy[2],Hussain Soliman[3]

[1],[2]Department of Mathematics, Sharnbasva University, Kalaburagi

[3]Department of Basic Science, Engineering Division,

International Academy for Engineering and Media Science, Egypt.

Corresponding author: kalyanshreedevi@gmail.com

Hussein.AbdAllah.Soliman@iaems.edu.eg

Abstract:

This paper investigates mass and thermal transfer in a system of infinite vertically parallel plates under the influence of a chemical reaction(first order). This setup involves a Casson fluid and immiscible fluids. Using perturbation techniques, we solve the nonlinear coupled mathematical model, applying appropriate restrictions. The incompressible fluids, is assumed, fluid have different viscosities and thermal conductivities, and their transport properties are considered constant. We match the separate solutions using appropriate matching conditions. The study analysis explores how various parameters affect heat and mass transfer, presenting the results graphically. We find that both the thermal & the mass Grashof numbers increase the flow. regardless of the presence of a first-order chemical reaction. While viscous dissipation, viscosity, width and conductivity ratio promote the flow, the first-order chemical reaction parameter tends to suppress it in both regions.

1. **Introduction:**

Convective flows play a crucial role in various industrial advantages, some of them are fiber and granular insulation and geothermal systems. Casson fluid, a type of non-Newtonian fluid with yield stress, is particularly significant. For instance, human blood act like a Casson fluid due to the presence of blood cells and substances like protein and fibrinogen. This characteristic makes the study of Casson fluid relevant in both scientific and engineering fields. Analyses of convective flows often include scenarios like free and mixed convection and

.

examine conditions with either symmetric or asymmetric heating. Typically, numerical techniques are used to analyze developing flows, as noted in reference [1], while fully developed flows are often examined analytically [2], and experimental data are also available [3].

The impact of viscous dissipation on the natural and forced convection in porous media has been explored by Ingham et al. [4]. More recent research, such as by Nield [5] and Magyari et al. [6], delves into the effects of viscous dissipation & buoyancy. Barletta et al. [7] provided Taylor series solutions analytical for mixed convection under isoflux-isothermal wall conditions. These studies generally focus on single-fluid models.

In contrast, many challenges in fields like petroleum engineering, geophysics, plasma physics, and magneto-fluid dynamics involve the flow of multiple fluids. Understanding importantance of immiscible fluid in drug engineering and medicine [8]. Various studies were explored the hydrodynamic aspects of 2-fluid flow. For example, Bird et al. [9] derived an exact solution. Bhattacharya [10] examined the flow of two immiscible fluids between rigid parallel plates. Examples underscore the necessity of understanding the dynamics of multiphase immiscible flows for accurate process modelling.

Modelling multi-fluid systems introduces complexities, especially concerning the transport phenomena. There has been both theoretical and practical research in horizontal pipes [11, 12]. Kumar et al. [13, 14] investigated convective immiscible fluids in channels. Barletta et al. [15] applied similar approaches to mixed convection channel flow of clear fluids under symmetric isothermal-isothermal wall conditions.

The study of two-fluid and thermal transfer is critical in the chemical and nuclear industries. These processes are particularly important for designing heat transport systems in space applications, where understanding thermal and diffusion transfer under reduced gravity is essential. Key aspects for designing two-fluid systems include identifying fluid flow regions, calculating pressure drops, assessing void fractions and quality reactions, and determining heat transfer coefficients for both fluids.

.

Malashetty and Leela [16] were investigated the Hartmann flow behaviour of two fluids. Further, the dynamics of two-phase flow & thermal transfer had examined by Malashetty and Umavati [17] and in other studies by Malashetty and colleagues [18, 19].

In this paper, we present analytical results concerning the fully-developed convective flow of a micropolar flow within a porous medium.

2. Mathematical Formulation

The first $(-h_1 \le Y \le 0)$ passage is occupied by Cassono fluid and the second passage $(0 \le Y \le h_2)$ is occupied by viscous fluid having different density, viscosity, thermal conductivity, thermal and concentration expansion ratios. Except the density all fluid properties are maintained constant.

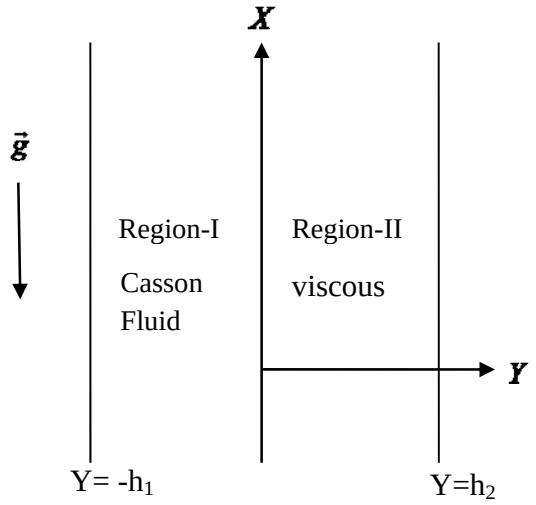

Fig.1 Mathematical formulation

Momentum, thermal and diffusion equations under the assumptions are given as fallows

Region-I

$$g\beta_{T1}(T_1 - T_{w2}) - \frac{1}{\rho_1}\frac{\partial p}{\partial X} + \nu(1+\frac{1}{\beta})\frac{d^2U_1}{dY^2} + g\beta_{C1}(C_1 - \overline{C}_2) - \frac{\sigma B^2 U_1}{\rho_1} = 0 \qquad (1)$$

$$K_1\frac{d^2T_1}{dY^2} + \mu_1\left(\frac{dU_1}{dY}\right)^2\left(1+\frac{1}{\beta}\right) = 0 \qquad (2)$$

.

$$D_1 \frac{d^2 C_2}{dY^2} - K_1 \left(C_1 - \overline{C_2} \right) = 0 \qquad (3)$$

Region-II

$$\rho_2 g \beta_{T2} (T_2 - T_{w2}) - \frac{\partial p}{\partial X} + \mu_2 \frac{d^2 U_2}{dY^2} + \rho_2 g \beta_{C2} (C_2 - \overline{C}_2) = 0 \qquad (4)$$

$$K_2 \frac{d^2 T_2}{dY^2} + \mu_2 \left(\frac{dU_2}{dY} \right)^2 = 0 \qquad (5)$$

$$D_2 \frac{d^2 C_2}{dY^2} - K_2 \left(C_2 - \overline{C_2} \right) = 0 \qquad (6)$$

Boundary conditions on the flows are

$$U_1(-h_1) = 0 ; \qquad U_2(h_2) = 0 ; \qquad U_1(0) = U_2(0) ; \qquad S\mu_1 \frac{dU_1}{dY}(0) = \mu_2 \frac{dU_2}{dY}(0) , T_2(h_2) = Tw_2 ,$$

$$T_1(-h_1) = Tw_1 \quad T_1(0) = T_2(0) , \qquad \kappa_1 \frac{dT_1}{dY}(0) = \kappa_2 \frac{dT_2}{dY}(0)$$

$$C_1(-h_1) = \overline{C_1} ; \quad C_2(h_2) = \overline{C_2} ; \quad C_1(0) = C_2(0) ; \qquad D_1 \frac{dC_1}{dY}(0) = D_2 \frac{dC_2}{dY}(0) \qquad (7)$$

Non-dimensional transformations

$$u_i = \frac{U_i}{\overline{U_1}} \quad , \quad y_i = \frac{Y_i}{h_i} \quad , \quad \theta_1 = \frac{T_1 - T_{w2}}{T_{w1} - T_{w2}} \quad , \quad \theta_2 = \frac{T_2 - T_{w2}}{T_{w1} - T_{w2}} \quad , \quad \phi_1 = \frac{C_1 - \overline{C_2}}{\overline{C_1} - \overline{C_2}} \quad , \quad \phi_2 = \frac{C_2 - \overline{C_2}}{\overline{C_1} - \overline{C_2}} \quad ,$$

$$Gr = \frac{g \beta_{T1} h_1^{\,3} (T_{w1} - T_{w2})}{\upsilon_1^{\,2}}, \quad Gc = \frac{g \beta_{C1} h_1^{\,3} \left(\overline{C_1} - \overline{C_2} \right)}{\upsilon_1^{\,2}}, \quad \mathrm{Re} = \frac{\overline{U_1} h_1}{\upsilon_1}, \; H = \frac{n h_1}{\overline{U_1}} \; p = \frac{h_1^{\,2}}{\mu_1 \overline{U_1}} \frac{dp}{dX},$$

$$\alpha_1^{\,2} = \frac{\kappa_1 h_1^{\,2}}{D_1} \qquad (8)$$

Modified nondimensional system of equations are

Region-I

$$(1 + \frac{1}{\beta}) \frac{d^2 u_1}{dy^2} + \lambda_1 \theta_1 + \lambda_2 \phi_1 - M^2 u_1 - p = 0 \qquad (9)$$

$$\frac{d^2 \theta_1}{dy^2} + Br \left(\frac{du_1}{dy} \right)^2 \left(1 + \frac{1}{\beta} \right) = 0 \qquad (10)$$

.

$$\frac{d^2\phi_1}{dy^2} - \alpha_1^2\phi_1 = 0 \qquad (11)$$

Region-II

$$\frac{d^2u_2}{dy^2} + \lambda_1\, mnh^2\, b_t\, \theta_2 + \lambda_2\, mnh^2\, b_c\, \phi_2 - mh^2 p = 0 \qquad (12)$$

$$\frac{d^2\theta_2}{dy^2} + \frac{KBr}{m}\left(\frac{du_2}{dy}\right)^2 = 0 \qquad (13)$$

$$\frac{d^2\phi_2}{dy^2} - \alpha_2^2\phi_2 = 0 \qquad (14)$$

The non-dimensional form of wall restrictions,

$$u_1(y) = 0, at\ y = -1 \quad ; \quad u_2(y) = 0, at\ y = 1 \quad ; \quad u_1(y) = u_2(y), at\ y = 0 \quad ;$$

$$S\mu_1 \frac{du_1}{dy}(y) = \mu_2 \frac{du_2}{dy}(y), at\ y = 0 \quad ; \quad \theta_1(y) = 1 at\ y = -1 \quad , \quad \theta_2(1) = 0 \quad , \quad \theta_1(0) = \theta_2(0) \quad ;$$

$$\frac{d\theta_1}{dy}(y) = \frac{1}{k\,h}\frac{d\theta_2}{dy}(y)\, at\ y = 0 \quad ; \quad \phi_1(-1) = 1 \quad ; \quad \phi_2(1) = 0 \quad ; \quad \phi_1(0) = \phi_2(0) \quad ;$$

$$\frac{d\phi_1}{dy}(y) = \frac{d}{h}\frac{d\phi_2}{dy}(y)\, at\ y = 0 \qquad (15)$$

where

$$GR_T = \frac{Gr}{\mathrm{Re}},\ GR_C = \frac{Gc}{\mathrm{Re}},\ h = \frac{h_2}{h_1},\ m = \frac{\mu_1}{\mu_2},\ b_t = \frac{\beta_{T2}}{\beta_{T1}},\ n = \frac{\rho_2}{\rho_1},\ b_c = \frac{\beta_{C2}}{\beta_{C1}},\ d = \frac{D_2}{D_1}.$$

3. Method of solutions

Non-linear and coupled equations are solved by regular perturbation technique and closed form solutions cannot be obtained. However, by assuming Brinkman number as small perturbation, we get the approximate analytical solutions.

$$\text{“}u_i(y) = u_{i0}(y) + \varepsilon u_{i1}(y) + \varepsilon^2 u_{i2}(y) + \ldots\text{”} \qquad (16)$$

$$\text{“}\theta_i(y) = \theta_{i0}(y) + \varepsilon\theta_{i1}(y) + \varepsilon^2\theta_{i2}(y) + \ldots\text{”} \qquad (17)$$

Equating the co-efficient of like powers of Br to zero and one we get equations as shown below

Region I

Zeroth order equations

.

$$\frac{d^2\theta_{10}}{dy^2} = 0 \tag{18}$$

$$(1+\frac{1}{\beta})\frac{d^2u_{10}}{dy^2} + \lambda_1\theta_{10} + \lambda_2\phi_1 - M^2u_{10} - p = 0 \tag{19}$$

First order equation

$$\frac{d^2\theta_{11}}{dy^2} + \left(\frac{du_{10}}{dy}\right)^2\left(1+\frac{1}{\beta}\right) = 0 \tag{20}$$

$$(1+\frac{1}{\beta})\frac{d^2u_{11}}{dy^2} + \lambda_1\theta_{11} - M^2u_{11} = 0 \tag{21}$$

Region II

Zeroth order equations

$$\frac{d^2\theta_{20}}{dy^2} = 0 \tag{22}$$

$$\frac{d^2u_{20}}{dy^2} + \lambda_1\, m\, n\, h^2\, b_t\, \theta_{20} + \lambda_2\, m\, n\, h^2\, b_c\, \phi_2 - m\, h^2\, p = 0 \tag{23}$$

First order equation

$$\frac{d^2\theta_{21}}{dy^2} + \frac{K}{m}\left(\frac{du_{20}}{dy}\right)^2 = 0 \tag{24}$$

$$\frac{d^2u_{21}}{dy^2} + \lambda_1\, m\, n\, h^2\, b_t\, \theta_{21} = 0 \tag{25}$$

Boundary conditions are:

$$u_{10}(y) = 0, at\ y = -1 u_{20}(y) = 0, at\ y = 1, u_{10}(y) = u_{20}(y), S\mu_1\frac{du_{10}}{dy}(y) = \mu_2\frac{du_{20}}{dy}(y), at\ y = 0,$$

$$\theta_{10}(-1) = 1, \theta_{20}(-1) = 1, \theta_{10}(0) = \theta_{20}(0),\ \frac{d\theta_{10}}{dy}(0) = \frac{1}{k\,h}\frac{d\theta_{20}}{dy}(0). \tag{26}$$

$$u_{11}(y) = 0, at\ y = -1, u_{21}(y) = 0, at\ y = 1, u_{11}(y) = u_{21}(y), S\mu_1\frac{du_{11}}{dy}(y) = \mu_2\frac{du_{21}}{dy}(y), at\ y = 0,$$

$$\theta_{11}(-1) = 1, \theta_{21}(-1) = 1, \theta_{11}(0) = \theta_{21}(0),\ \frac{d\theta_{11}}{dy}(0) = \frac{1}{k\,h}\frac{d\theta_{21}}{dy}(0). \tag{27}$$

The solutions for concentrations are directly obtained

.

$$\phi_1 = A_1 Cosh(\alpha_1 y) + A_2 Sinh(\alpha_1 y) \quad (28)$$

$$\phi_2 = A_3 Cosh(\alpha_2 y) + A_4 Sinh(\alpha_2 y) \quad (29)$$

Flow solutions are displayed as below

$$\theta_{10} = c_1 y + c_2$$

$$\theta_{20} = c_3 y + c_4$$

$$u_{10}(y) = B_1 Cosh(Zy) + B_2 Sinh(Zy) + ry + r_1 + r_2 Cosh(\alpha_1 y) + r_3 Sinh(\alpha_1 y)$$

$$u_{20}(y) = A_6 + A_5 y + r_4 y^2 + r_5 y^3 + r_6 Cosh(\alpha_2 y) + r_7 Sinh(\alpha_2 y)$$

$$\theta_{11}(y) = A_8 + A_7 y + T_5 Cosh(2\alpha_1 y) + T_6 Cosh(\alpha_1 y) + T_7 Cosh(\alpha_1 y) Cosh(Zy) + T_8 Cosh(\alpha_1 y) Sinh(Zy) + T_9 y^2 + T_{10} Cosh(Zy) + T_{11} Cosh(2Zy) + T_{12} Sinh(Zy) + T_{13} Sinh(2Zy) + T_{14} Sinh(\alpha_1 y) + T_{15} Cosh(Zy) Sinh(\alpha_1 y) + T_{16} Sinh(Zy) Sinh(\alpha_1 y) + T_{17} Sinh(2\alpha_1 y)$$

$$\theta_{21}(y) = A_{10} + A_9 y + T_{18} y^2 + T_{19} y^3 + T_{20} y^4 + T_{21} y^5 + T_{22} y^6 + T_{23} Cosh(y\alpha_2) + T_{24} y Cosh(y\alpha_2) + T_{25} y^2 Cosh(y\alpha_2) + T_{26} Cosh(2\alpha_2 y) + T_{27} Sinh(\alpha_2 y) + T_{28} y Sinh(\alpha_2 y) + T_{29} y^2 Sinh(y\alpha_2) + T_{30} Sinh(2\alpha_2 y)$$

$$u_{11}(y) = B_3 Cosh(Zy) + B_4 Sinh(Zy) + r_8 + r_9 y + r_{10} y^2 + r_{11} Cosh(2\alpha_1 y) + r_{12} Sinh(2\alpha_1 y) + r_{13} Cosh(\alpha_1 y) + r_{14} Sinh(\alpha_1 y) + r_{15} Cosh(2Zy) + r_{16} Sinh(2Zy) + r_{17} Cosh([\alpha_1 + Z] y) + r_{18} Cosh([\alpha_1 - Z] y) + r_{19} Sinh([\alpha_1 + Z] y) + r_{20} Sinh([\alpha_1 - Z] y) + r_{21} Sinh([\alpha_1 + Z] y) + r_{22} Sinh([\alpha_1 - Z] y) + r_{23} Cosh([\alpha_1 + Z] y) + r_{24} Cosh([\alpha_1 - Z] y) + r_{25} y Cosh(Zy) + r_{26} y Sinh(Zy)$$

$$u_{21}(y) = A_{12} + A_{11} y + r_{23} y^2 + r_{24} y^3 + r_{25} y^4 + r_{26} y^5 + r_{27} y^6 + r_{28} y^7 + r_{29} y^8 + r_{30} Cosh(y\alpha_2) + r_{31} y Cosh(y\alpha_2) + r_{32} y^2 Cosh(y\alpha_2) + r_{33} Cosh(2y\alpha_2) + r_{34} Sinh(y\alpha_2) + r_{35} y Sinh(y\alpha_2) + r_{36} y^2 Sinh(y\alpha_2) + r_{37} y^2 Sinh(2y\alpha_2)$$

4. Results and discussion

The differential equations (9)–(14) describing the flow of an incompressible Casson fluid between two vertical plates have been analytically solved under the given restrictions (15). The solutions, expressed in closed form (18) to (25), are illustrated graphically. The velocity and microrotation components are plotted for various parameters.

.

Figures 2a and 2b depict the influence of the mixed convection parameter (GR_T) on velocity and temperature. Enhances in (GR_T) enhances the buoyancy force, thus aiding fluid motion, especially noticeable in the micropolar flow compared to the porous region, as shown in Figure 2b. However, as (GR_T) increases, the microrotation velocity diminishes. If the micropolar fluid is substituted with a viscous fluid, the impact of the thermal Grashof number persists, though the enhancement is more pronounced in viscous incompressible fluids than in micropolar fluids.

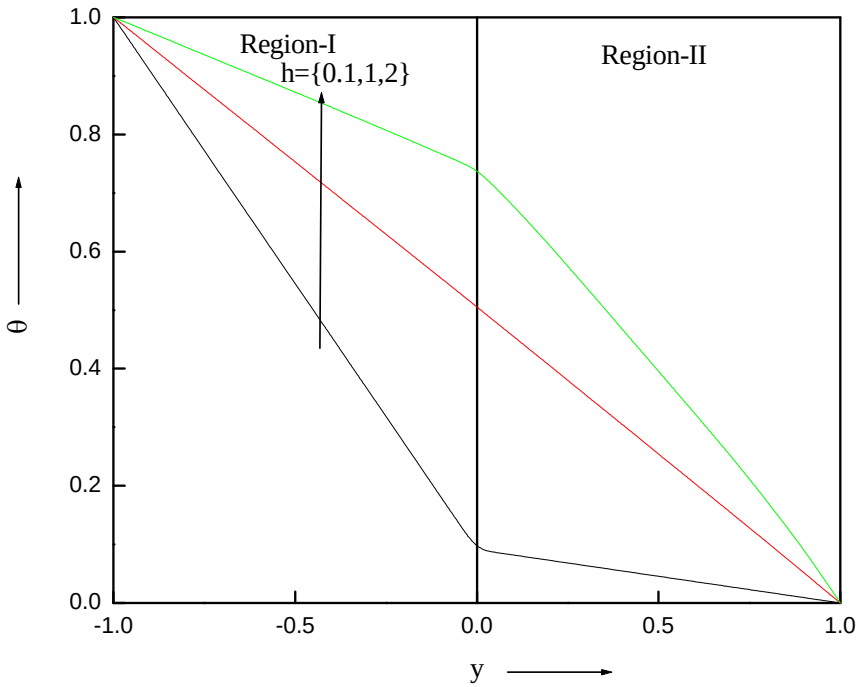

Fig. 2a. Tempreture profile for different values of width ratio h.

.

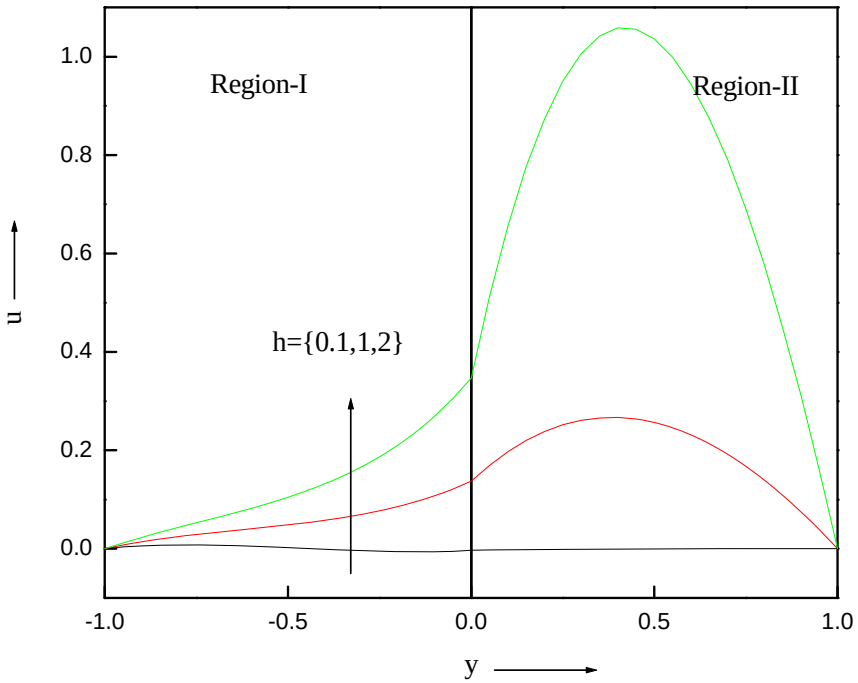

Fig. 2b. Velocity profile for different values of width ratio h.

.

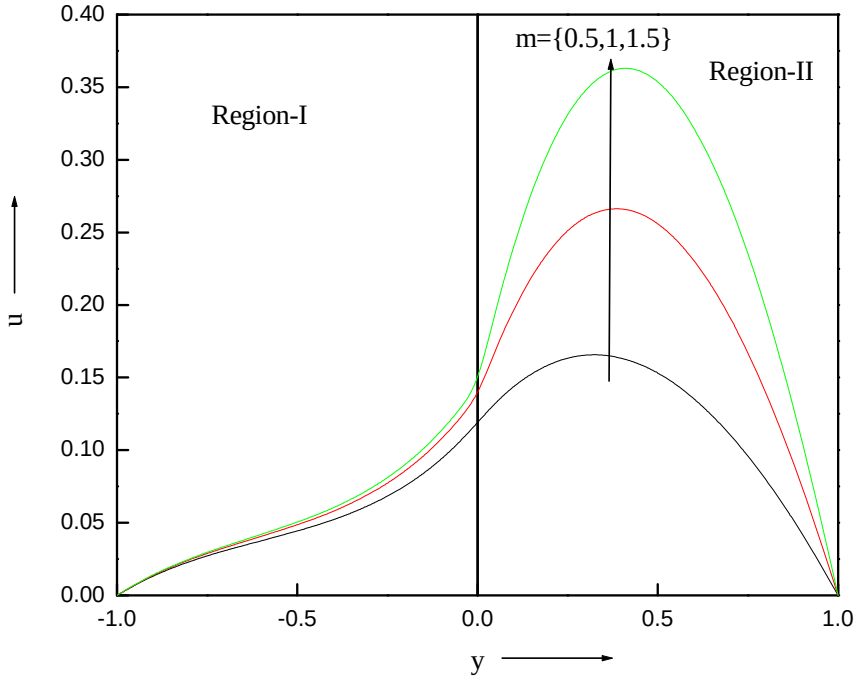

Fig.3a.Velocity profile for different values of viscocity ratio m.

.

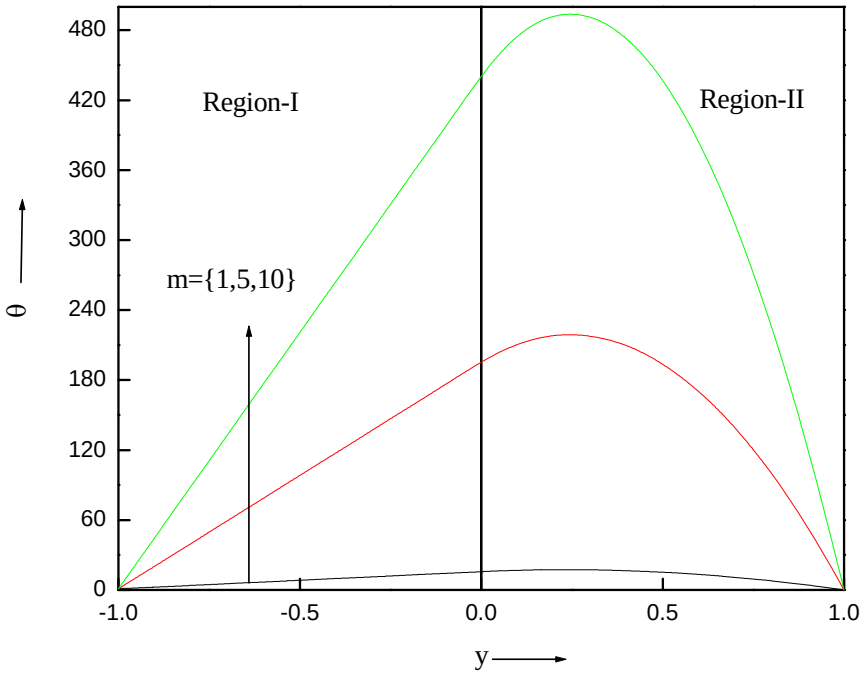

Fig.3b.Temperature profile for different values of viscocity ratio m.

.

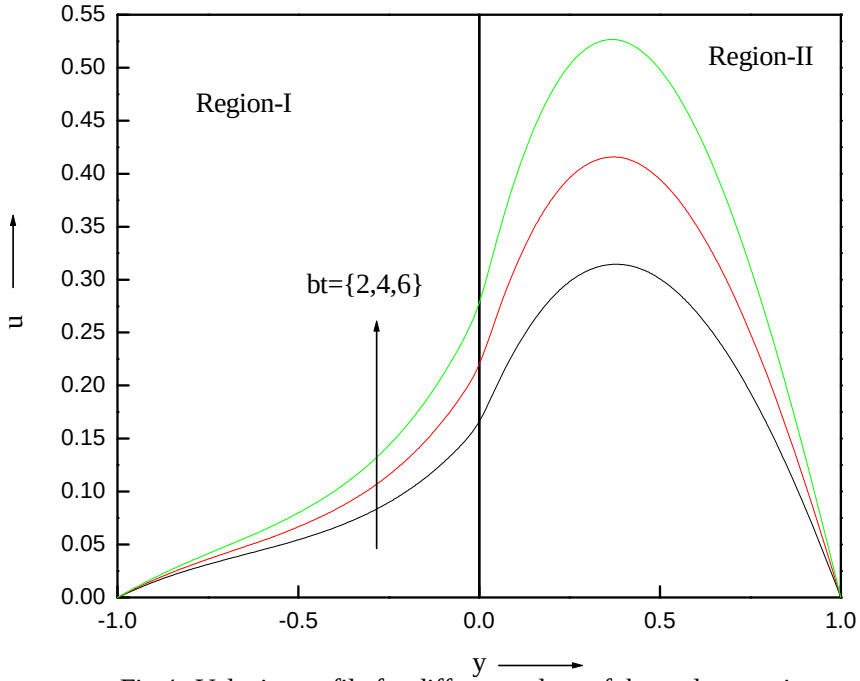

Fig.4a.Velocity profile for different values of thermal expansion coefficient ratio bt.

.

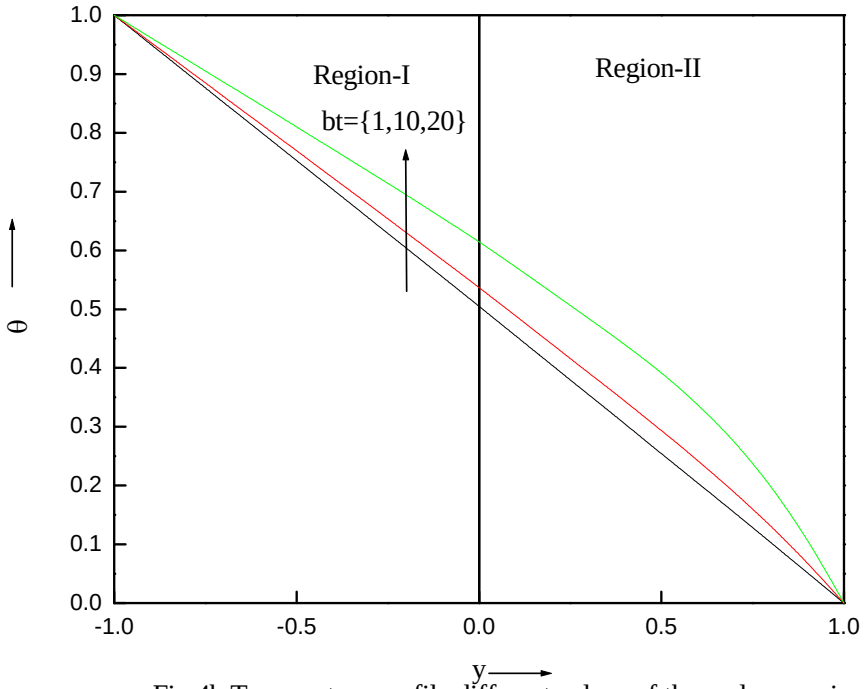

Fig.4b.Temperature profile different values of thermal expansion coefficient ratio bt.

.

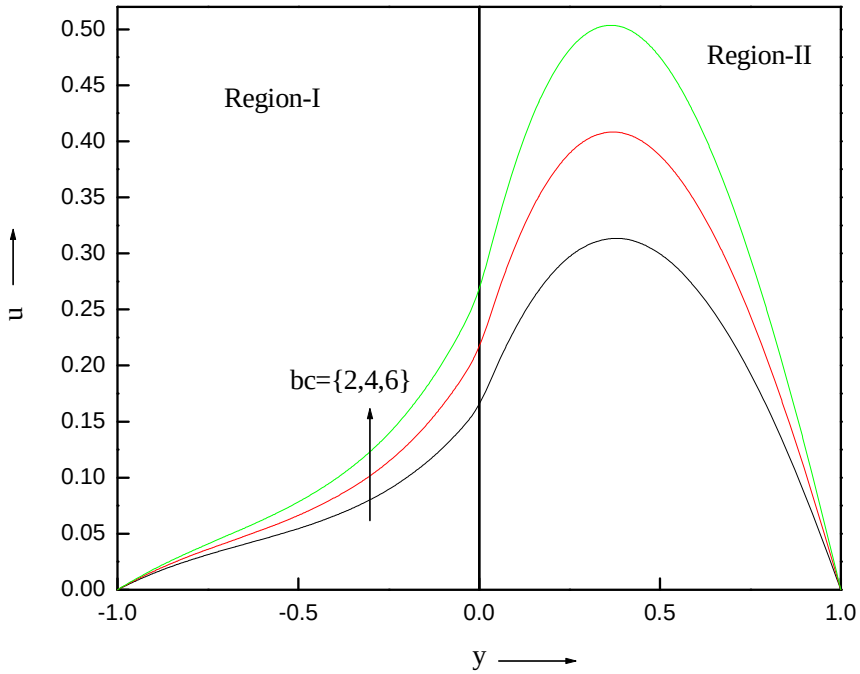

Fig.5a.Velocity profile for different values of concentration expansion ratio bc.

.

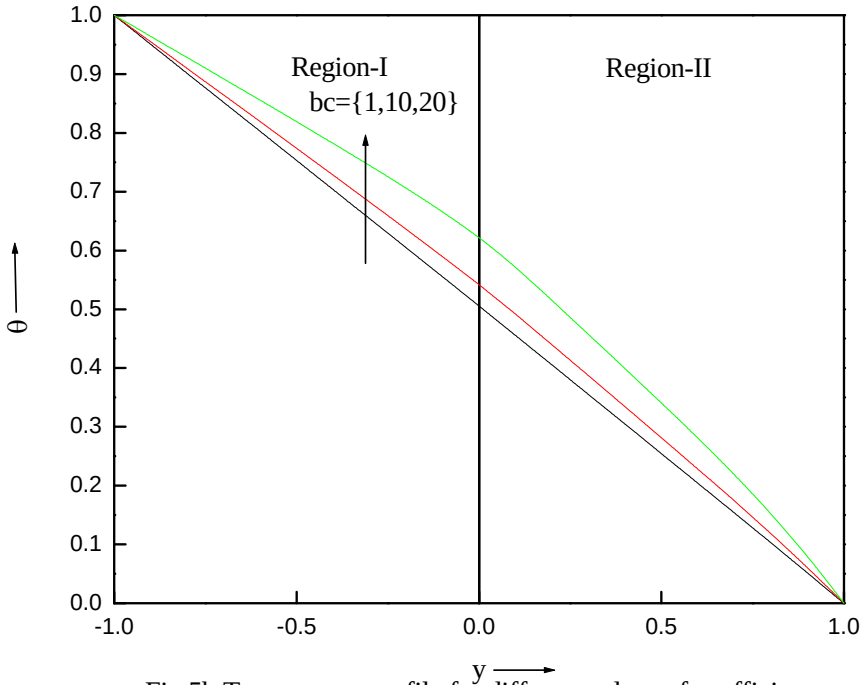

Fig.5b.Temperature profile for different values of coefficients concentration expansion ratio bc.

.

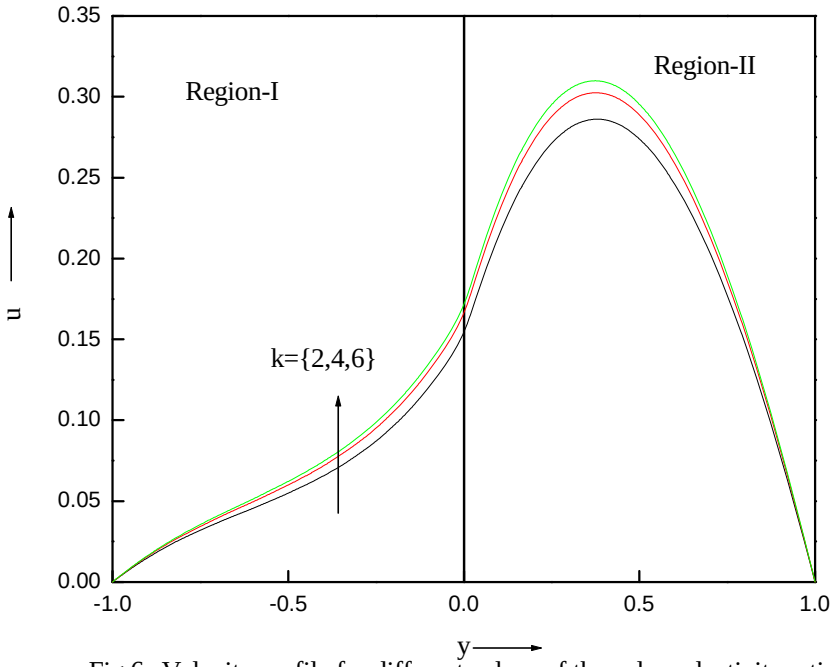

Fig.6a.Velocity profile for different values of themal conductivity ratio k.

.

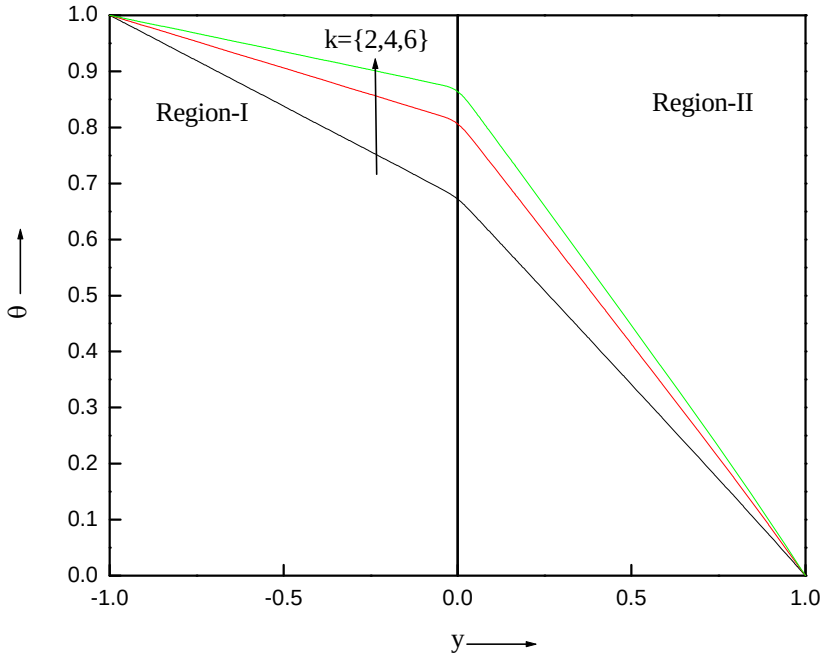

Fig.6b.Temperature profile for different values of thermal conductivity ratio k.

.

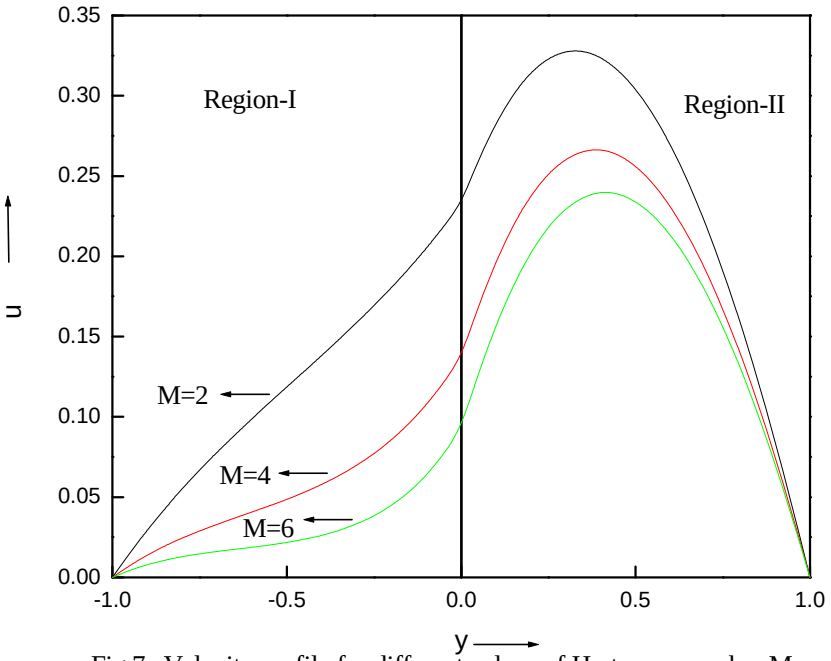

Fig.7a.Velocity profile for different values of Hartmann number M.

.

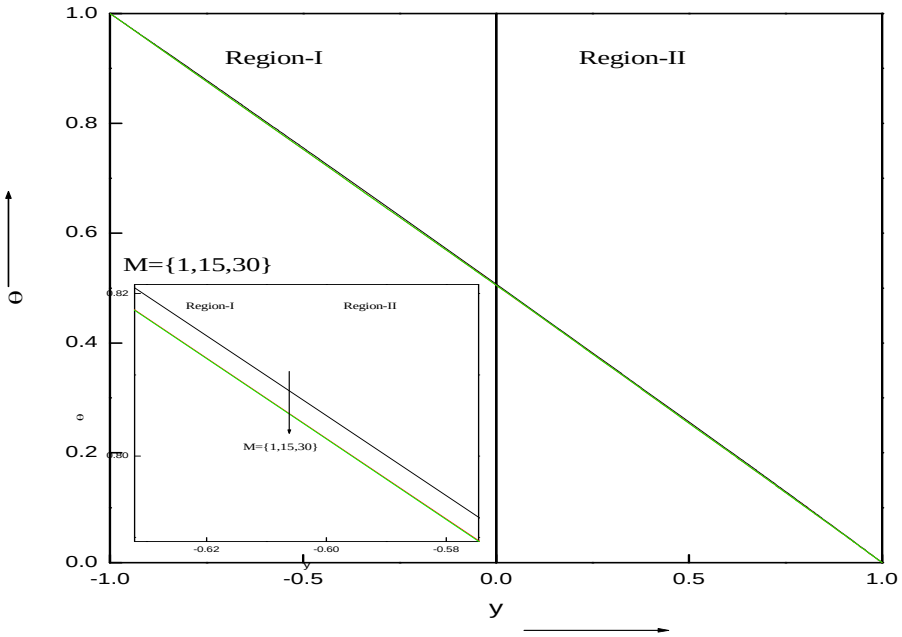

Fig.7b.Temperature profile for different values of Hartmann number M.

.

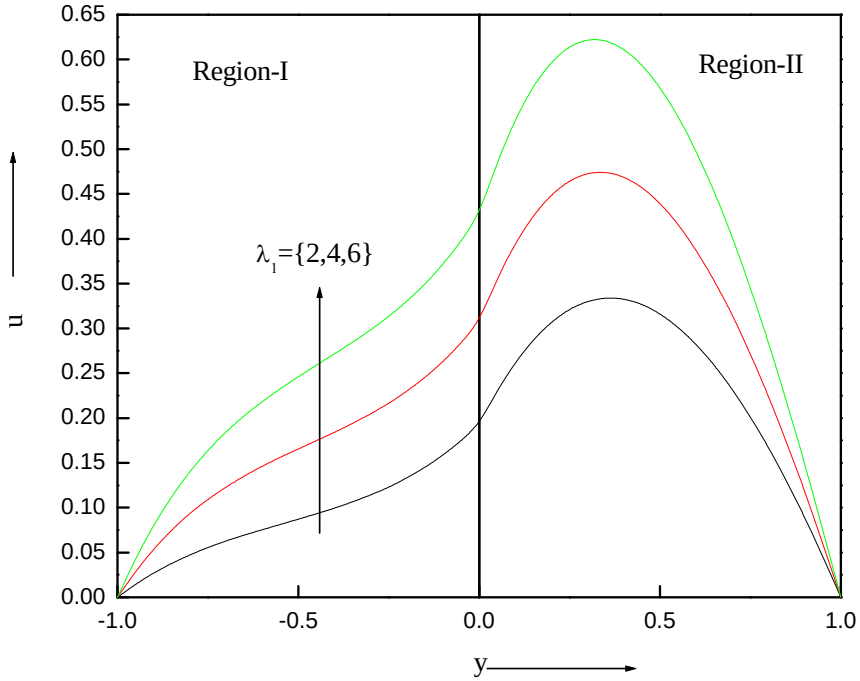

Fig.8a.Velocity profile for different value of λ_1.

.

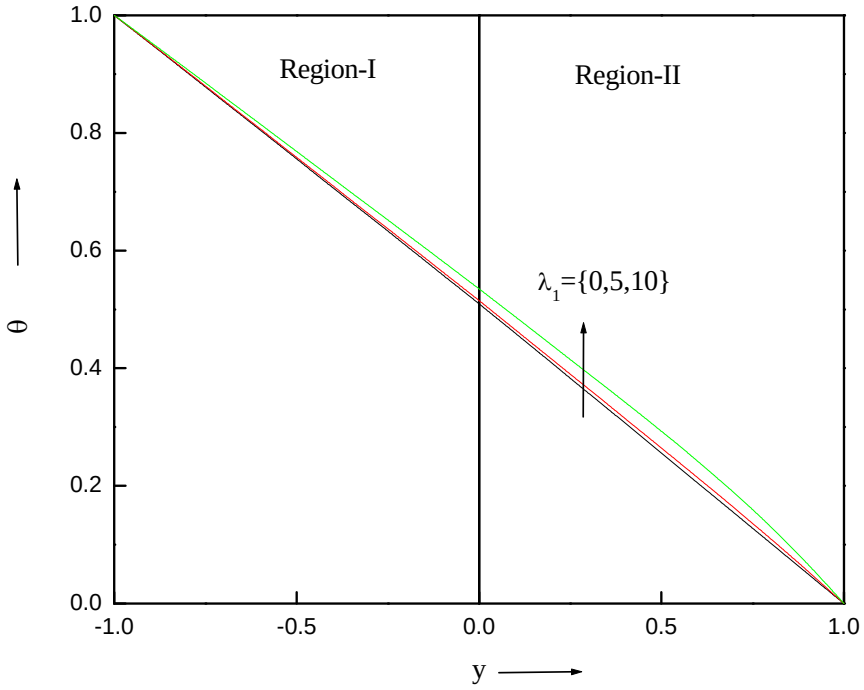

Fig.8b.Temperature profile for different values of λ_1

.

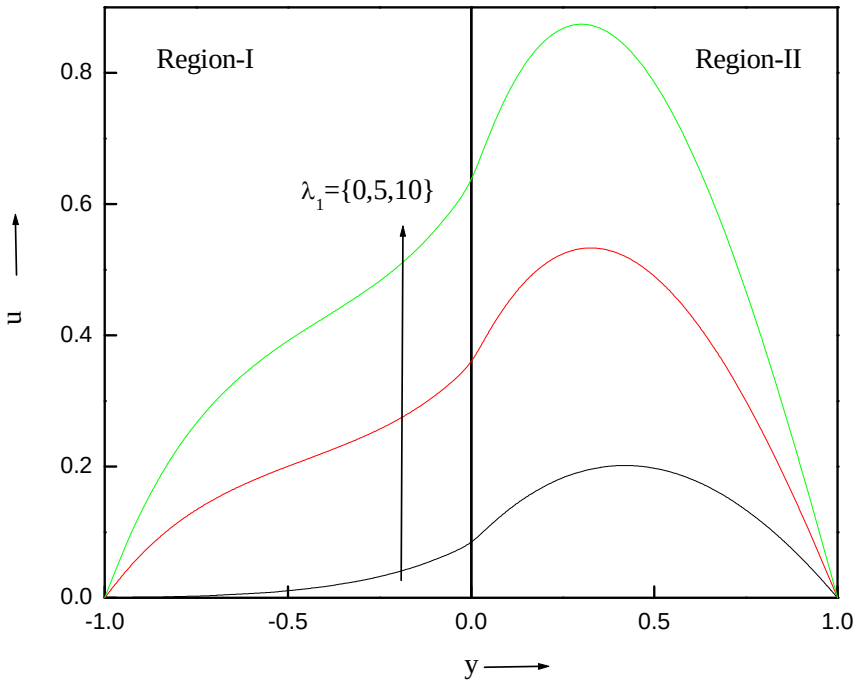

Fig.9a.Velocity profile for different values of λ_2.

.

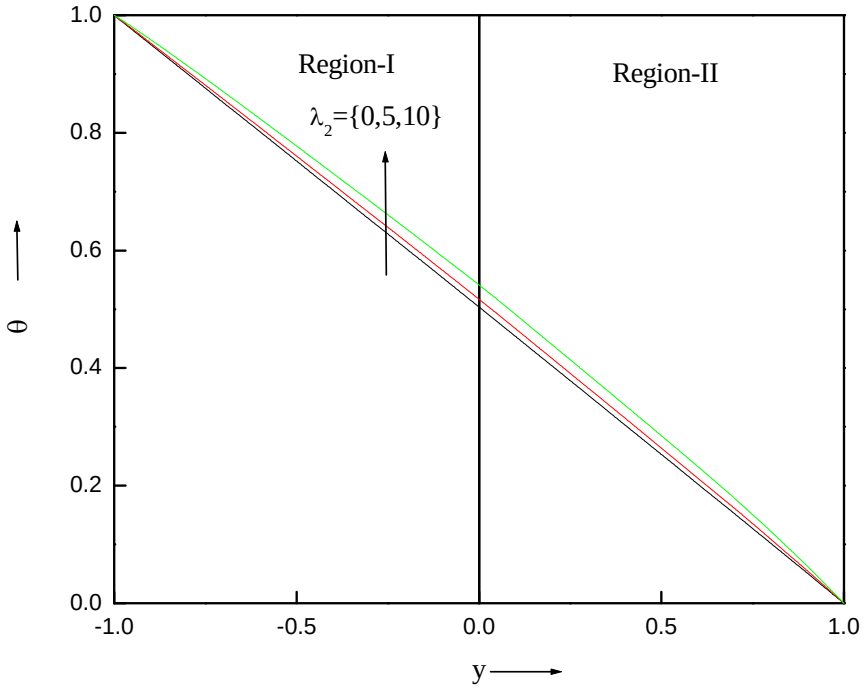

Fig.9b.Temperature profile for different value of λ_2.

.

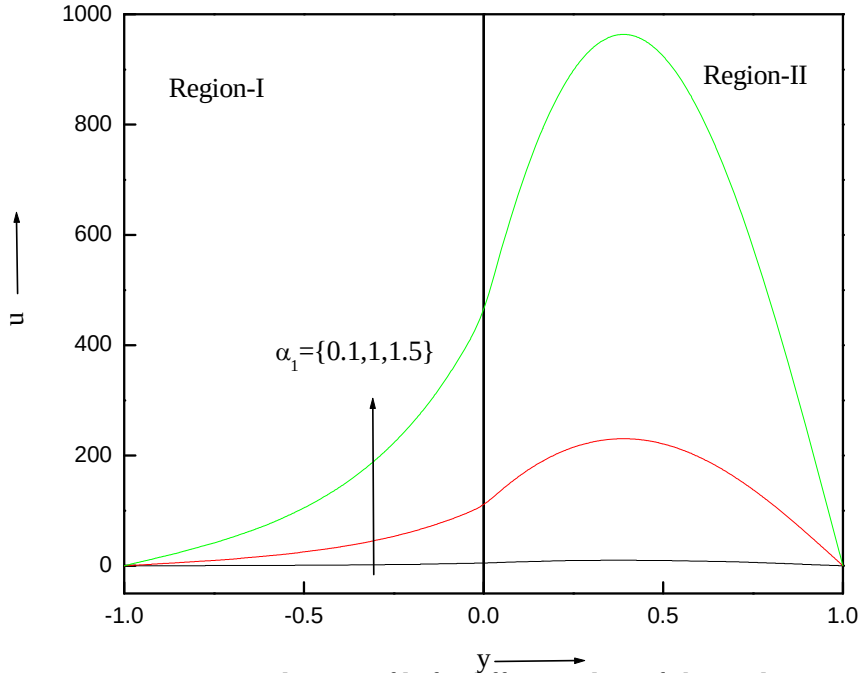

Fig.10a.Velocity profile for different values of chemical reaction parameter α_1.

.

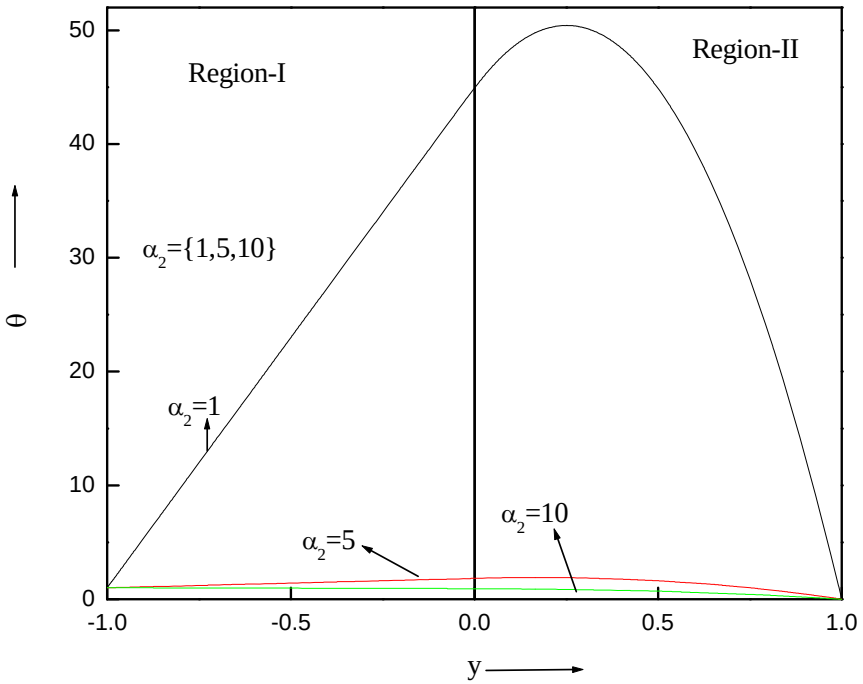

Fig.10b.Temperature profile for different values of chemical reaction parameter α_1.

.

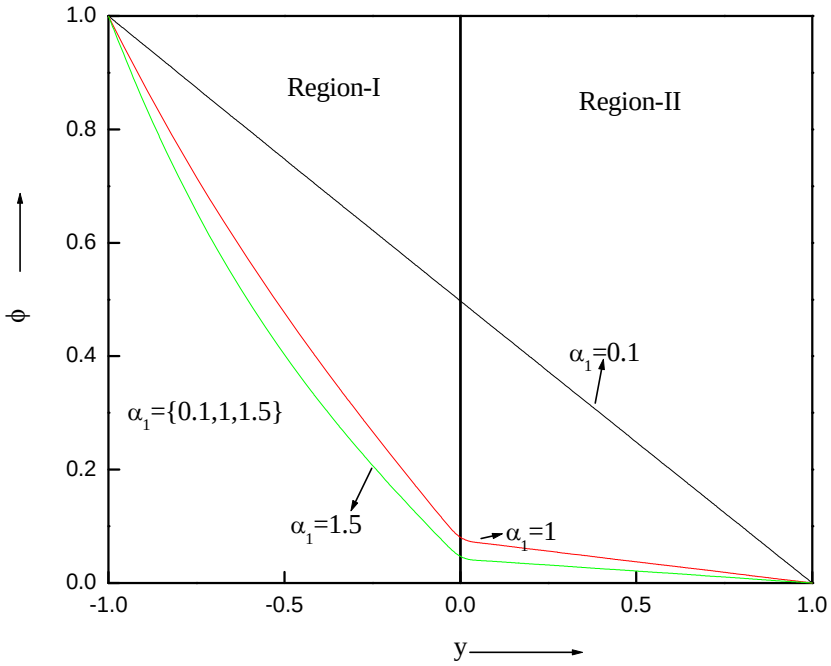

Fig.10c.Concentration profile for different values of chemical reaction parameter α_1.

.

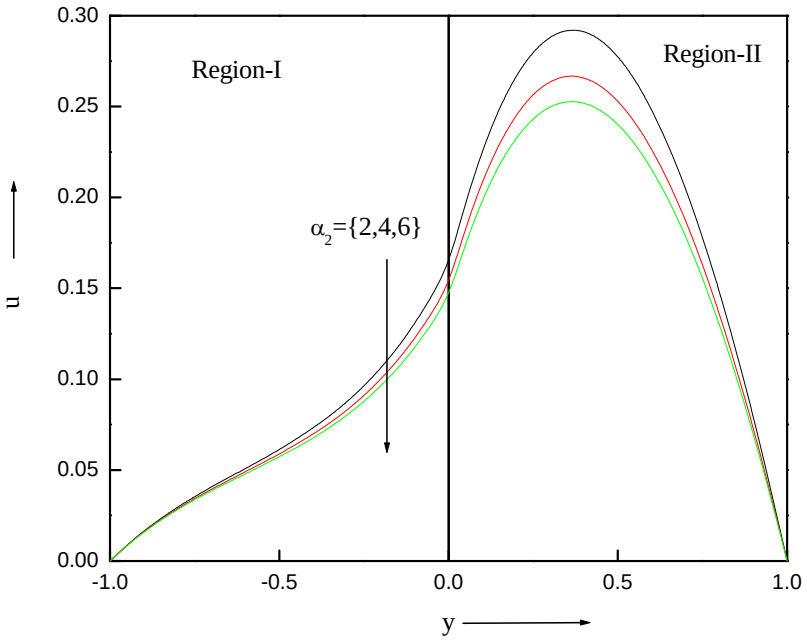

Fig.11a.Velocity profile for different values of chemical reaction parameter α_2.

.

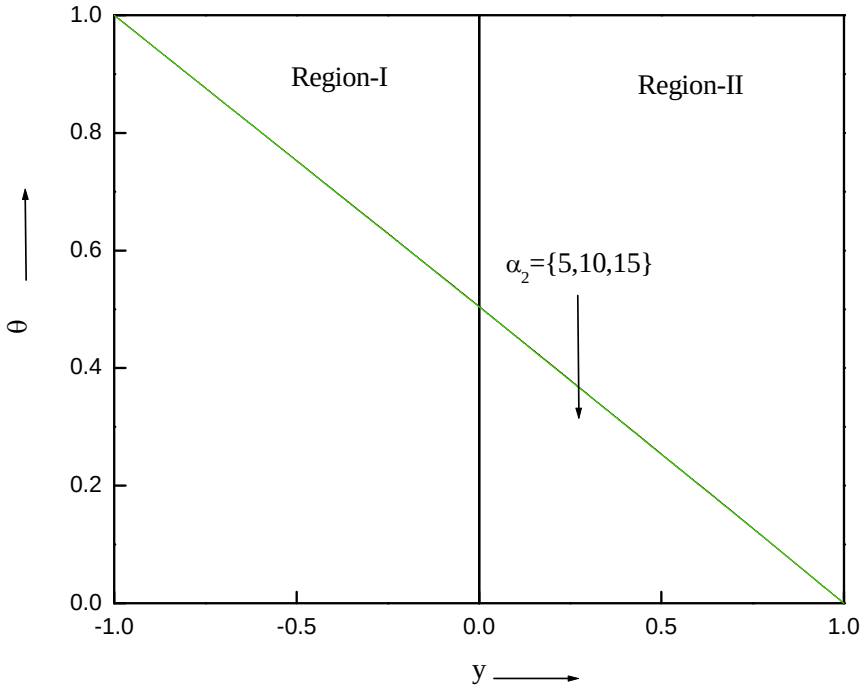

Fig.11b.Temperature profile for different values of chemical reaction parameter α_2.

.

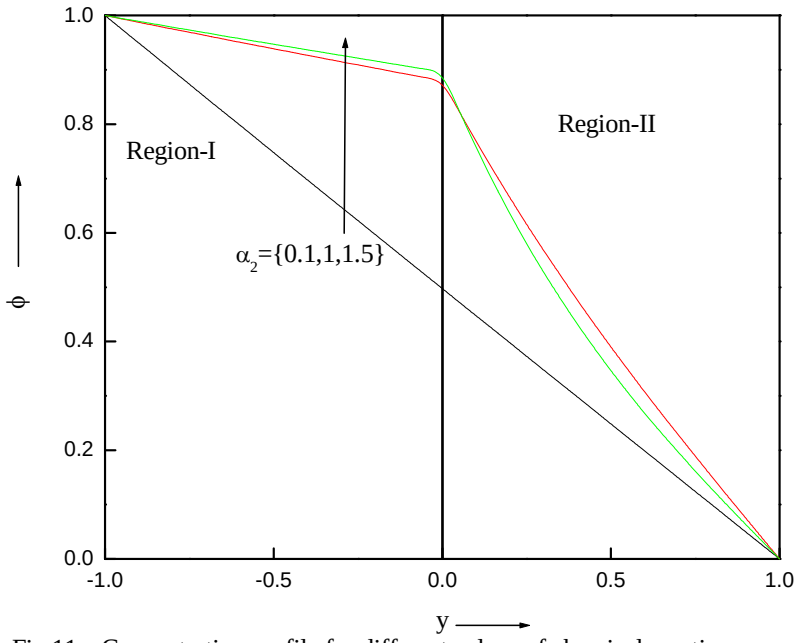

Fig.11c. Concentration profile for different values of chemical reaction parameter α_2.

Conclusions:

The following conclusions are drawn

- Higher thermal and mass Grashof numbers lead to an increase in both velocity and temperature within the system.
- An enhancement in the viscosity, width, and conductivity ratio results in a corresponding enlargement of the flow field.
- The flow field diminishes when a first-order chemical reaction is present, compared to when it is absent. Additionally, as the rate of the chemical reaction increases, both thermal and concentration transfer tend to diminished.

.

- An increase in modified Grashof number, viscosity , width, and conductivity ratio contributes to higher volumetric flow rates, species concentrations, and heat addition to the flow.
- The discrepancy between analytical and numerical solutions grows as the Brinkman number increases.

References:

[1] E. Daria, S. Kimura and A. Okajima: Natural convection heat transfer in an asymmetrically heated vertical channel controlled by through flows. JSME Ser. B, vol. 41, pp. 227-232, 1998.

[2] T. T. Hamadah and R. A. Wirtz: Analysis of laminar fully developed mixed convection in a vertical channel with opposing buoyancy. ASME .J. Heat Transf., vol.113, pp.507-510, 1991.

[3] E. M. Sparrow, J. M. Chrysler, and L. F. Azevedo: Observed flow reversals and measured – predicted Nusselt numbers for natural convection in a one-sided heated vertical channel. ASME. J. Heat Transfer, vol. 106, pp. 325-332, 1984. Open Journal of Heat, Mass and Momentum Transfer (2014) 28-46 45

[4] D. B. Ingham, I. Pop, and P. Cheng: Combined free and forced convection in a porous medium between two vertical walls with viscous dissipation. Transport in porous media, vol.5, pp. 381-398, 1990.

[5] D. A. Nield, Comments on 'A new model for viscous dissipation in porous media across a range of permeability values'. Transport in Porous Med., vol. 55, pp. 253- 254, 2004.

[6] E. Magyari, D. A. S. Rees, and B. Keller: Effect of viscous dissipation on the flow in fluid saturated porous media, in: K. Vafai (Ed.) Handbook of Porous Media, seconded. Taylor and Francis, New York, pp. 373-406, 2005.

[7] A. Barletta, E. Magyari, and B. Keller: Dual mixed convection flows in a vertical channel. Int. J. Heat Mass Transfer, vol. 48, pp. 4835-4845, 2005.

[8] E. E. Tzirtzilakis: A mathematical model for blood flow in magnetic field. Physics of Fluids, vol. 17, Issue 7, pp. 077103/1–077103/15, 2005.

[9] R. B. Bird, W. E. Stewart, and E. N. Lightfoot: Transport phenomena., Wiley, New York, 1960.

.

[10] R. N. Bhattacharya: The flow of immiscible fluids between rigid plates with a time dependent pressure gradient. Bulletin of the Calcutta Mathematical Society, vol. 1, pp. 129–137, 1968.

[11] S. Alireza and V. Sahai: Heat transfer in developing magnetohydrodynamic Poiseuille flow and variable transport properties. International Journal of Heat and Mass Transfer, vol. 33, pp. 1711–1720, 1990.

[12] M. S. Malashetty and V. Leela: Magnetohydrodynamic heat transfer in two phase flow. International Journal of Engineering Sciences, vol. 30, pp. 371–377, 1992.

[13] J. PrathapKumar, J. C. Umavathi, and M. Biradar. Basavaraj: Mixed convection of magnetohydrodynamic and viscous fluid in a vertical channel. International Journal of Non-Linear Mechanics, vol.46, pp.278–285, 2011.

[14] J. C. Umavathi, J. PrathapKumar, and M. Shekar: Convective flow between a corrugated and a smoothwall. Journal of porous media, vol.15 (10), pp.975–988, 2012.

[15] A. Barletta, E. Magyari, I. Pop, and L. Storesleten: Mixed convection with viscous dissipation in a vertical channel filled with a porous medium. Acta Mechanica, published online, April 19, pp.123-140, 2007.

[16] M. S. Malashetty and V. Leela: Magnetohydrodynamic heat transfer in two phase flow. International Journal of Engineering Sciences, vol. 30, pp. 371–377, 1992.

[17] J. PrathapKumar, J. C. Umavathi, and M. Biradar. Basavaraj: Mixed convection of magnetohydrodynamic and viscous fluid in a vertical channel. International Journal of Non-Linear Mechanics, vol.46, pp.278–285, 2011.

[18] J. C. Umavathi, J. PrathapKumar, and M. Shekar: Convective flow between a corrugated and a smoothwall. Journal of porous media, vol.15 (10), pp.975–988, 2012.

[19] G. S.Beavers and D. D. Joseph: Boundary conditions at naturally permeable wall. J. Fluid Mech, vol. 13, pp.197-207, 1967.